

# CORE AND EXPERIMENTAL FACILITIES CHARACTERISATION DURING THE COMMISSIONING OF THE ETRR-2 REACTOR

G. Gennuso<sup>1</sup>, C. Leco<sup>2</sup>, Amr Abdelhady<sup>3</sup>

## **Abstract**

The ETRR-2 is a 22 MW reactor, MTR type, which was critical at November of 1997

During the commissioning of the ETRR-2 reactor core, neutron measurements were made in order to test some parameters to comply with the technical acceptance requirements. Power peaking factor was one of the measured parameters through density power estimation. It was estimated through a flux mapping with gold diluted activation detectors and calculated results. Around sixty points of the core in the refrigeration channels between fuel plates were instrumented to place gold detectors (bare and under Cd). The agreements between experimental and calculated results allow calculating with low error the power peaking factor defining a correction factor for correct the calculated value with the experimental determination. The obtained value for the Power Peaking Factor was 2.4 ( $\pm 0.20$ )

In the design of the core it was stipulated a minimum average flux in the cobalt facility. Activation detectors were used to test the average flux in the Cobalt facility. A special device for low flux perturbation was placed in the facility having detectors in seventy-two positions. The comparison with calculations showed good agreement in the average flux and in the point flux too.

## **INTRODUCTION**

The ETRR-2 is a 22 MW research reactor and it reached its first criticality on November 1997. In February 1998 was assembled the operation core. In this core were made the experiences to measure the power peaking factor and the thermal average flux in the cobalt irradiation device. Both experiences are part of the technical guarantee procedures of the reactor and the experiences weren't part of a research plan. So, it imposed two important conditions to the measurements: a) short time to obtain results and b) quality assurance in the procedures.

### ***ETRR2 Description***

The ETRR-2 fuel is MTR type with 19 fuel plates. Fuel elements can be placed in different arrangements. The basic geometric unit in the X-Y core array is a square of 8.1x8.1 cm<sup>2</sup>. It can house an 8.0x8.0 cm<sup>2</sup> fuel element, an empty box or an irradiation device. As it is shown in Figure 1, inside the chimney there is a 30-position grid with a 6x5 configuration. Around the chimney there is an external grid array. The external grid has locations where reflectors, empty boxes and irradiation devices can be placed. Graphite thermal column and beryllium block are both divided into a set of

---

independent reflectors and a solid block. Six Ag-In-Cd control and safe plates are disposed dividing the core as is shown in Figure 1. A second shutdown system composed of four chambers that may be filled by injection of Gadolinium surround the core. The reactor has three-operation regimes: free convection (regime 0), forced convection-one pump (Regime 1), and forced convection-two pumps (Regime 2). In regime 0 the maximum power is 400 kW, in regime 1 is 10 Mw and in regime 2 is 22MW. In forced convection the flow circulation is upward, which is the reason of the existence of a chimney. The irradiation grid has independent refrigeration with flow circulation downward.

The operation core was named 2/98 and its configuration is showed in Figure1. This core had three types of fuel with different Uranium content, in order to simulate the equilibrium configuration The Type 1 fuel has 146 gr. of Uranium, the Type 2 fuel has 210 gr. and the Normal fuel has 405 gr. The core is reflected by Beryllium. Figure 1 shows the irradiation places inside the core for cobalt and in the external grid.

### ***Calculation codes***

To obtain the power peaking factor and the average thermal flux in the cobalt box results obtained by calculations were used. These results were used previous to the irradiation to predict the detector locations, and after the irradiation to correlate the experimental data in order to obtain those factors.

The calculation method is divided in two steps:

- a) Cell calculation: It is used to calculate macroscopic cross sections of different materials for the core calculation.
- b) Core calculation: It is used to calculate neutronic parameters of the core as neutron fluxes, power and burnup distribution, reactivities, peaking factor, cycle length, kinetic parameters, etc.

All the codes used belong to the MTR\_PC system and they are:

- 1) The nuclear data library used for calculation was the original WIMS library with updates from ENDF/B-IV of Ag, In, Cd, and Gd.<sup>8</sup>
- 2) WIMS<sup>9</sup>. The collision probabilities option in one dimensional geometry (slab) is used for cell calculation.
- 3) POS\_WIMS<sup>10</sup>. This program is used to homogenise and condense macroscopic XS from WIMS calculation.
- 4) CITVAP 3.1<sup>11</sup>. It is a core diffusion code. It is a new version of CITATION II program.
- 5) HXS 4.1<sup>12</sup>. It is the macroscopic cross section library manager program. It is used for the interface between cell and core calculation.

### ***Calculation models***

For the evaluation of the cell constants the WIMS code is used in slab geometry. The results of WIMS calculations are processed in different ways to obtain the core constants for the different materials.

The core calculation is performed with the CITVAP diffusion code in x-y-z with an energy discretization of three groups :

Group 1 : 10.000 MeV -> 0.821 MeV  
Group 2 : 0.821 MeV -> 0.625 eV  
Group 3 : 0.625 eV -> 0.000 eV

A conceptual description of the most important core components is given in the following subsections.

### ***Standard Fuel Element***

The macroscopic XS of the whole standard fuel element is homogenised after a WIMS calculation.

### ***Control Element Zone***

The control rod zone is divided in different zones at core level calculation:

1. A zone of Aluminium and water outside the active width of the absorber, corresponding to the ends of the guide box.
2. If the absorber rod is in, there is a homogenised zone of Aluminium, water, stainless steel, Helium and Ag-In-Cd. It was verified by core calculations that a homogenisation of all the zones inside and including the guide plates is good enough for control rod worth calculation.
3. If the absorber plate is out, the space it leaves in the guide box is occupied by the follower rod (coupling rod). The model has two homogeneous regions:
  - a. The zone outside of the follower: Aluminium and water.
  - b. The follower zone: Aluminium, water and stainless steel.

### ***Gadolinium Injection Zone***

The gadolinium injection zone is divided in different zones at core level calculation:

- a) The corner of the chimney: which is made of pure Zircalloy. Some Zircalloy is not considered in the calculation.
- b) The horizontal faces (see figure 1) of the chimney have different water gaps than the vertical ones. This is approximated by averaging the water gaps.

## **POWER PEAKING EVALUATION**

The measurement of Power Peaking Factor is extremely difficult to be made directly. To measure the average thermal flux in the core we need, in fact, measure a huge quantity of points and determine the point of maximum thermal flux. Then, an approximation is necessary to be made: to measure a number of points and correlate it with a shape of the flux. It has the difficulty of assuming separability in X, Y and Z directions, which is not really true.

Another way to do this is measure several points in order to have a sampling and compare it with calculation. If this comparison shows a good agreement, statistically measurable, we can use the calculated data distribution corrected by

some experimental factor that take in account the differences between calculated and experimental data. Therefore it is necessary to choose the points carefully so we have information about the more relevant zones in the core. This option was adopted for the Power Peaking Factor evaluation.

### **Experimental method**

The measured points were chosen from a previous calculated flux mapping. Thermal activity was measured assuming a Maxwellian shape of the flux in the thermal range. Bare and under Cadmium diluted Gold-Al wires were used as detectors. The evaluated Cadmium Factor is 1.031<sup>(1,2)</sup>. Flux depression was estimated according to Reference (3) and no corrections were necessary.

Different mass fuel, position near control rod, positions near reflector and near irradiation cobalt-box were mapped. Cadmium ratio ( $R_{Cd}$ ) was obtained for each zone.

The zone near the estimated peak of flux and peak of power was carefully mapped and special considerations were made in order to minimise the experimental error.

The samples were mounted on Aluminium plates inside numbered cavities (Figure 2). These plates were placed in channels between fuel plates. Special care was taken to assure the position of the plate in the core and the detectors in the plates. Three irradiations were necessary and all were made in Regime 0 of operation. Irradiation number 1 and 2 were made with bare detectors and irradiation number 3 with under Cadmium detectors. For points measured with bare detectors with estimated equal  $R_{Cd}$ , one or two of them were chose for measuring with under Cadmium detectors in order to reduce the measured points. Tables 1, 2 and 3 showed details of the each irradiation and the detector position in the plate and in the core.

### **Thermal Activity Determination**

Thermal activity for the samples was calculated in according to the Maxwellian model as <sup>(1)</sup>:

$$A_{th} = A_{bare} (1 - F_{Cd}/R_{Cd}) \quad \text{Equation 1}$$

The Cadmium Ratio  $R_{Cd} = A_{Bare}/A_{Cd}$  was used in the points were under Cadmium samples were not activated.

The saturated activity for sample irradiation is calculated as:

$$A_s = \frac{\lambda A_{Net} P_{dd}}{N_0 \lambda (1 - e^{-\lambda t_i})(1 - e^{-\lambda t_m}) e^{-\lambda t_w}} \quad \text{Equation 2}$$

where:

$\lambda$ : decay constant for Au<sup>197</sup>

$N_0$ : target nuclei of Au<sup>197</sup>

$A_{Net}$ : net photopeak counts

$P_i$ : power normalisation factor between irradiations. Assuming  $A_{s1}^M$  as the reference monitor, then

$$P_i = \frac{A_{s1}^M}{A_{si}^M} \quad \text{Equation 3}$$

and  $A_{si}^M$  is the saturated activity in the  $i$  irradiation.  $A_{s1}^M$  has the power information.

$g$ : yield branching for photopeak

$e$ : efficiency for gamma energy  $E_\gamma=411$  keV.

$dd$ : detector dead time correction factor given by

$$dd = \frac{(1 - e^{-t_m})(e^{-(t_m - t_i)} - 1)}{(1 - e^{-t_i})(t_m - t_L)} \quad \text{Equation 4}$$

$t_i$ : irradiation time

$t_w$ : waiting time between the end of the irradiation and the start of the counting.

$t_m$ : sample counting time

$t_L$ : system live time during the counting period

The irradiation time  $t_i$  was estimated so that the correction for the start-up time could be neglected. However, start-up signal of the fission counters were recorded in order to estimate the correction to be applied if it was necessary.

## Results

Usually a fresh core is built with only one type of fuel elements and the experimental measurement of the thermal flux distribution gives a very good estimation of the power distribution. The ETRR-2 2/98 core has three different types of fuel elements. The difference between fuel elements is the total mass of uranium. Therefore the flux distribution is strongly different than the power distribution.

Three options were investigated in order to obtain the power distribution through the thermal flux distribution measurements<sup>4</sup>

1. Validate calculation against measurement of the thermal flux and assume the same error in the distribution for the power distribution.
2. Measure the thermal flux and correct it using the thermal fission cross section of the homogeneous fuel element.
3. Measure the thermal flux and correct it using the total mass of  $U^{235}$  per fuel element.

The conclusion was that any of the three different approaches can be used to determine the power density distribution, anyway the third approach was suggested to be used, because it has no calculated parameter to adjust the measurement and the methodology error is lower than 8%. That means the following expression for the Power Peaking Factor

$$PPF = \frac{\int_r \frac{\phi(r) M(r)}{r} dr}{\int_r dr} \approx \frac{\sum_i \phi_i M_i V_i}{\sum_i V_i}$$

**Equation 5**

- $\phi$  = Thermal flux
- $M$  = Mass of the fuel  $i$
- $\phi_i$  = values of flux in  $i$  position of the fuel
- $M_i$  = Mass of the fuel in position
- $V_i$  = Volume element.

The measured results of thermal activity were obtained in the space between plates and it was compared with calculated fluxes in the fuel.

In Table 4 are presented the thermal activities, the normalised thermal activities and the normalised calculated flux. The normalisation in order to the comparison was made with the summation of thermal activities and calculated fluxes respectively. In Figure 3 is showed the comparison between experimental and calculated data for radial and axial planes.

The calculated data was obtained according to the procedure described above.

The  $\chi^2/N$  analysis to compare experimental and calculated data shows a value of 0.91 for a variance of 8% of experimental data and 10% in calculated data. It indicates statistically the agreement between experimental and calculated data. The flux peak and the power peak positions are in agreement.

Using the measured data a factor was calculated in order to correct the calculated power peaking factor. The methodology avoids using a volume element with the experimental data. The calculated flux in a volume where is the measurement point is compared with the experimental data. This factor measure the difference between calculated and experimental peaking factor for a sampling of points:

$$F_c = \left( \frac{(A_i M_i)_{i_{max}}}{\sum_i A_i M_i} \right)^{exp} * \left( \frac{\sum_i \phi_i M_i}{(\phi_i M_i)_{i_{max}}} \right)^{calc} \quad \text{Equation 6}$$

where  $i$  correspond to the experiment or calculated values in the  $i$  position and

- $\phi_i$  = Calculated values of flux in  $i$  position
- $A_i$  = Thermal activation in  $i$  position
- $M_i$  = Mass of the fuel in position  $i$

The correction factor value is  $F_c = 0.91 (\pm 0.07)$  and the calculated Power Peaking Factor ( $PPF_c$ ) is 2.66. Then the Peaking Factor is

$$PPF = PPF_c F_c = 2.66 \cdot F_c = 2.42 (\pm 0.20)$$

## **AVERAGE FLUX IN COBALT DEVICE**

Measurements of thermal neutron fluxes were made in the cobalt irradiation box in order to determine the average thermal flux in the active zone of the box. 0.112%Au diluted in Al activation wire detectors were placed in equidistant positions in a special device in order to use the same weighting volume for each point. The numbers of measured points were chosen taking in count these criteria:

- To minimise the flux perturbation between activation detectors
- To minimise the number of irradiations for reducing the error in the normalisation between different irradiations.
- The estimated difference for the average flux between the “infinite points” of measurements and sampling points lower or equal 5%. The infinite points measurement is called that hypothetical sampling made with a huge quantity of points.

## ***Experimental Method***

The core used for the measurement is the configuration 1/98. The only difference with the core 2/98 is that the cobalt device is out of the core. In this place was placed the measurement device. The irradiation box is in position D3 indicated in Figure 1.

Control Rod position for the irradiation were (little variations are recorded for different irradiations)

CR1: 100%	CR4: 22%
CR2: 100% (safety rod)	CR5: 100%(safety)
CR3: 0%	CR6: 0%

Three irradiations were needed for determine the average flux. The first and second irradiation were made at a low power for flux distribution determination, and the third was made at a power of  $2.5(\pm 4\%)MW$  in order to normalise the average value at this power.

A special device was used to locate the samples in the irradiation box. Seventy-two positions were mapped. The positions of the samples are equidistant in order to simplify the calculus of average flux weighting always with the same volume.

In figure 4 a schematic drawn of the device is shown. Additionally flux in the central point in the middle plane was measured. This point was used as normalisation between irradiations.

The irradiation time was 2:30 hr in the irradiations at low power and 1 hr in the high power irradiation.

0.112%Au diluted in Al activation Bare and under Cadmium detectors were irradiated.

Na-I(Tl) detector was used for activation determination of the detectors. The detector was previously calibrated in efficiency with a set of calibration source. The weight of each detector was used as normalisation. In the case of high flux irradiation the wire had to be cut in pieces for measuring activities and a special procedure was designed for extracting this detector from the device under water.

The start up time was corrected when it was necessary <sup>(5)</sup>.

### Thermal flux Results

Maxwellian shape of the flux was assumed in the thermal zone of the neutron spectrum <sup>(2,3)</sup>. This zone goes from 0 to 0.1 eV. It was calculated as:

$$f_{th} = \frac{A_{th}}{g^{Au}(T) \sqrt{\frac{293.6}{T}} \frac{\sqrt{\rho}}{2} S_{2200}^{Au} G_s} \quad \text{Equation 7}$$

where:

$A_{th}$ : saturated thermal activity

$$A_{th} = A_{Bare} - F_{Cd} A_{Cd} = A_{Bare} \left(1 - \frac{1}{R_{Cd}}\right)$$

$F_{Cd}$ : Cadmium factor

$R_{Cd}$ : Cadmium ratio =  $\frac{A_{Bare}}{A_{Cd}}$

$S_{2200}^{Au}$ : activation cross section of Gold at the energy 0.025 eV

$T$ : neutron temperature

$G_s$ : self shielding factor

$g(T)$ : factor that measure the departure of  $1/v$  in the cross section energy dependence.

The  $G_s$  factor<sup>(6)</sup> was set equal 1.0 for diluted gold in aluminium and the neutron temperature was referenced to the moderator temperature as proposed in /2/.

The constants used were:

Constant	value
$\sigma_{Au(2200)}$	98.65(±0.09) barn <sup>(6)</sup>
$I^\infty$	1562(±28) barn <sup>(6)</sup>
$F_{cd}$	1.031(±0.007) <sup>(1),(4)</sup>
$g(T)_{Au}$	1.0051 <sup>(1)</sup>
$T_{1/2}^{Au198}$	2.696(±0.002)days <sup>(7)</sup>

Saturated activities were estimated as referred in Equation 2, 3 ,4

For each plane of measurement Cadmium Ratio ( $R_{cd}$ ) was measured in two positions (center axial line and another point).

Table 5 shows the thermal flux in each plane for 2.5 MW. The data of thermal flux in each measured point are presented in table 6. The errors were estimated by propagation. The main source of error is in the efficiency of the detector followed by the mass weight.



The average flux in the Cobalt irradiation box is at 2.5 MW:

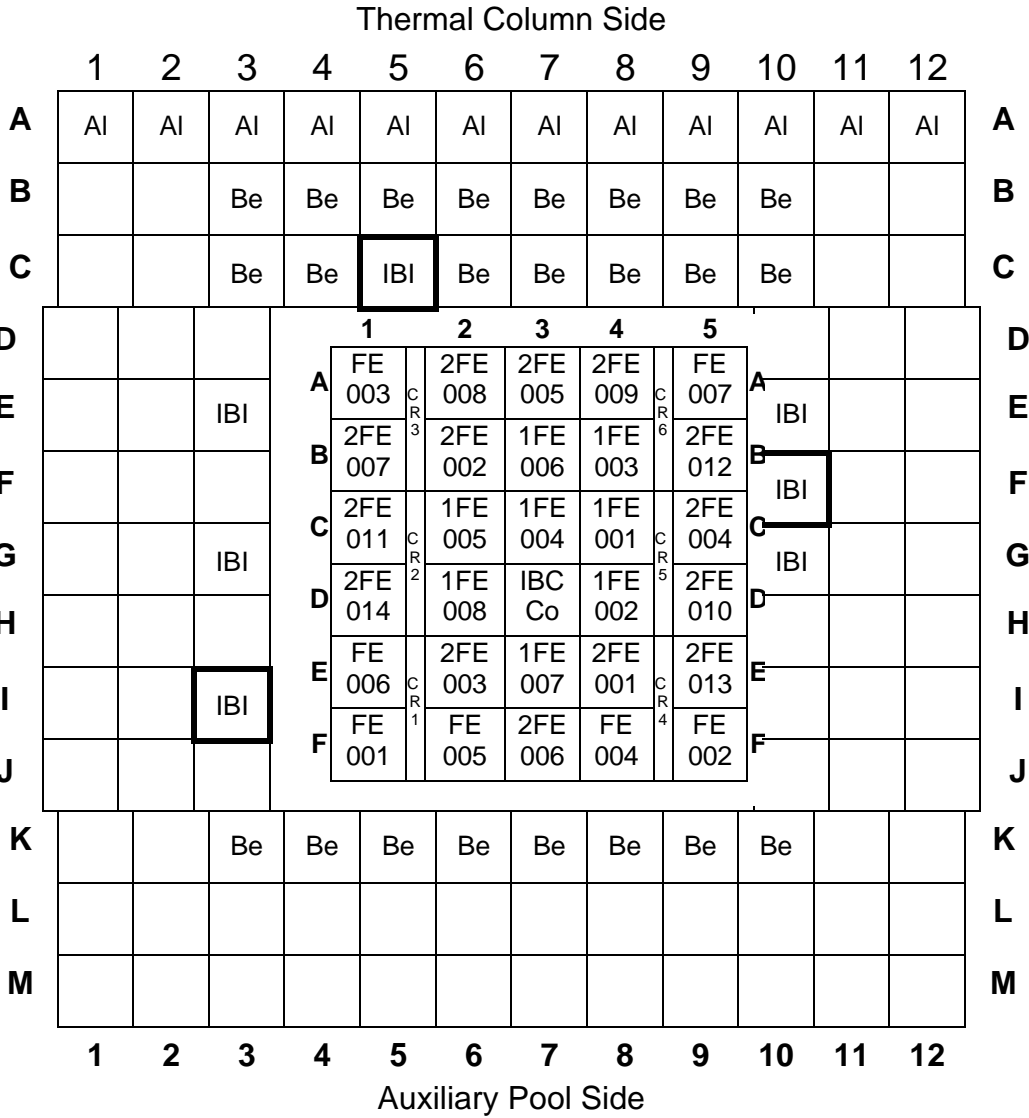
$$4.24 \cdot 10^{13} (\pm 3.5 \cdot 10^{12}) \text{ nv}$$

Then, at 22MW, the average flux in the irradiation box is

$$3.73 \cdot 10^{14} (\pm 2.9 \cdot 10^{13}) \text{ nv}$$

Comparisons between calculated and measured thermal flux are showed in Table 6. The differences between the average calculated value and the measured values are lower than 2%, in the case of the sampling, and 5% comparing with the calculated average value with huge quantity of points (referred previously as "infinite").  $\chi^2/N$  analysis was made between calculated and experimental values and a deviation that corresponds at a variance of 8% was found satisfactory. Figure 5 show the axial profile for two planes of measurement and Figure 5 the comparison between experimental and calculated data.

# Core 2/98



Fuel element Quantity: 29

Be Quantity: 23

FE xxx	Standard Fuel Element	1FE xxx	Type 1 Fuel Element	2FE xxx	Type 2 Fuel Element
IBC Co	Irradiation Box with Co	NS	Neutron Source	IBC	Irradiation Box. Core Grid
Al	Aluminum Block	Be	Beryllium reflector	IBI	Irradiation Box. Irradiation Grid
S Be	Special Beryllium	CPg	Core Plug	IPg	Irradiation Plug
<div style="border: 2px solid black; width: 20px; height: 20px; display: inline-block;"></div>	Fission Counter	CR	Control Rod No. n	<b>CR</b>	Safety Rod No. n

**Figure 1 Core configuration for the Core 2/98**

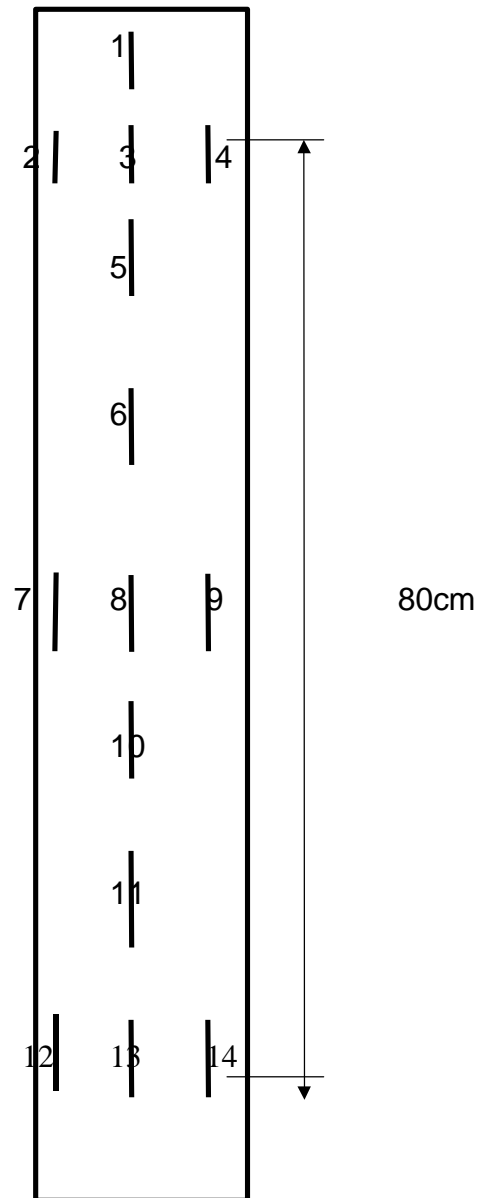


**Figure 2: Aluminium Plate for putting the detectors in the numbered cavities.**

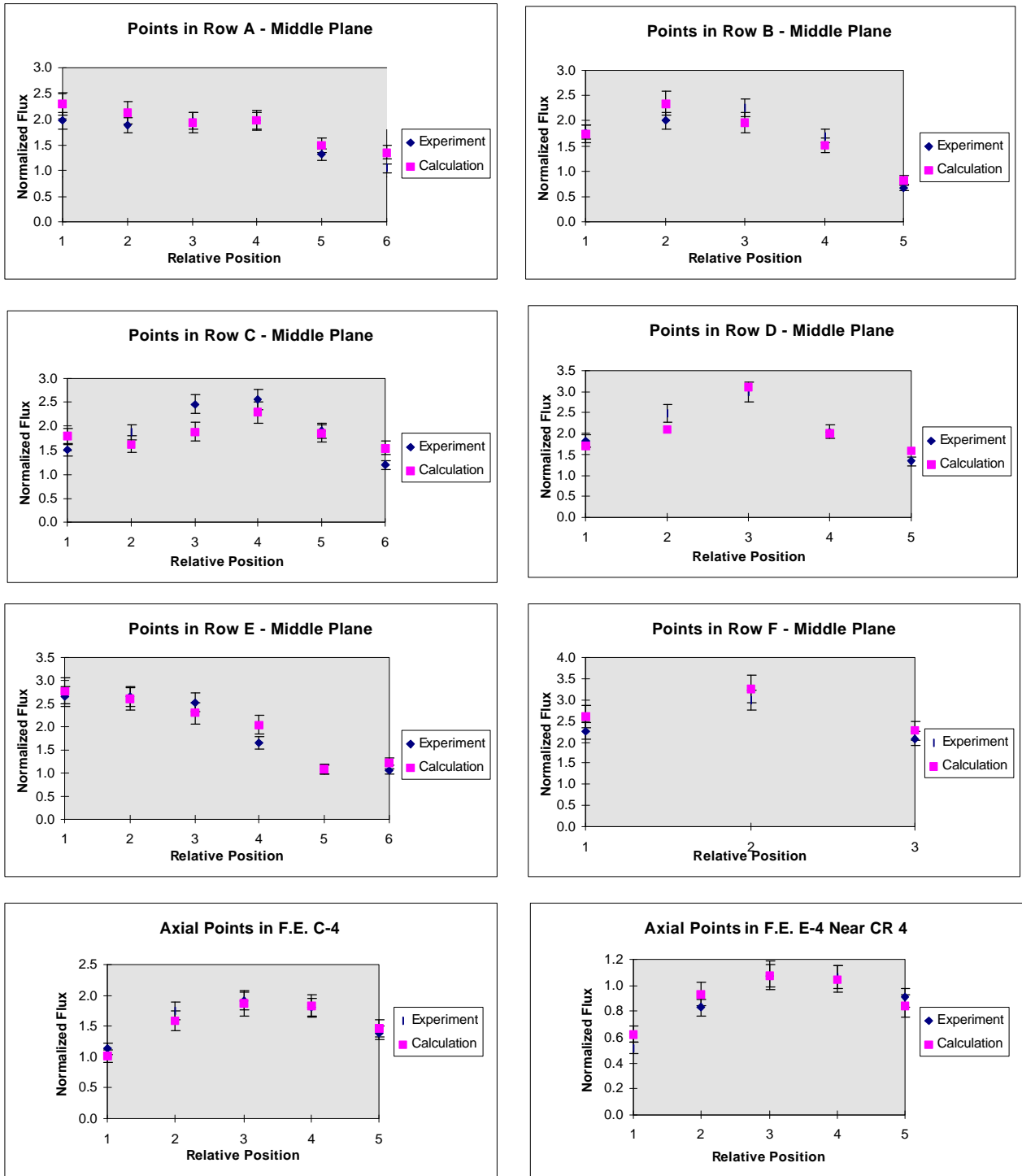
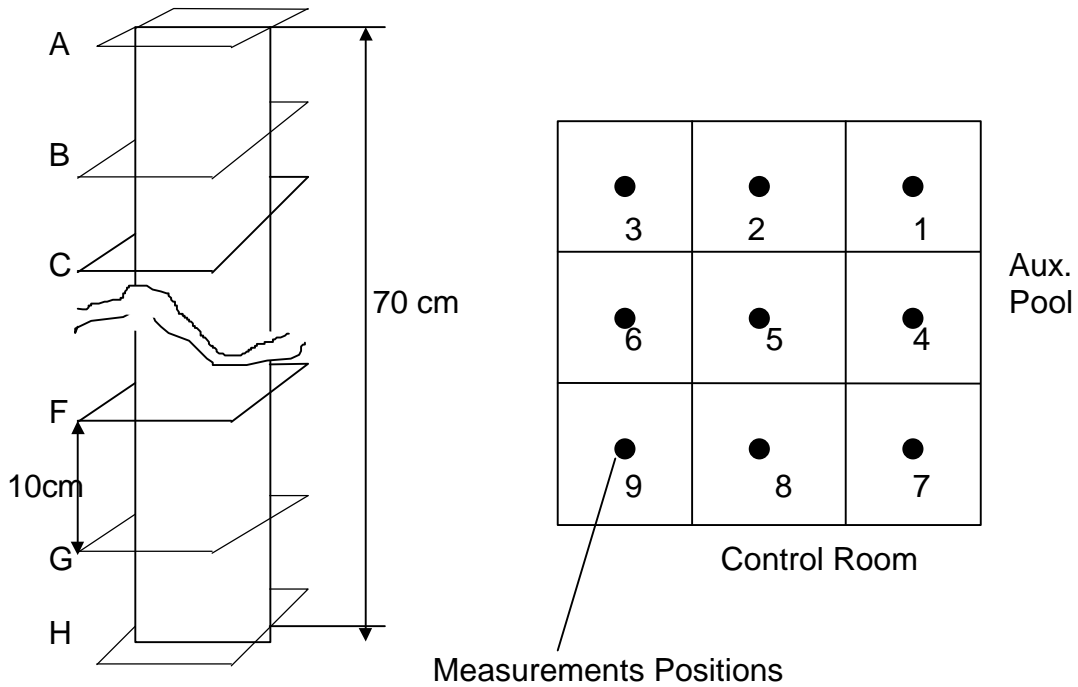


**Figure 3: Experimental and calculated values for different planes**



The Planes are labeled from A to H and the measurements positions in each plane for 1 to 9. The control Room and Aux. Pool in the draw indicate the position of the samples in the plane for identification in table 3 The device is centered in active length.

**Figure 4: Device for detector location in the cobalt-box**

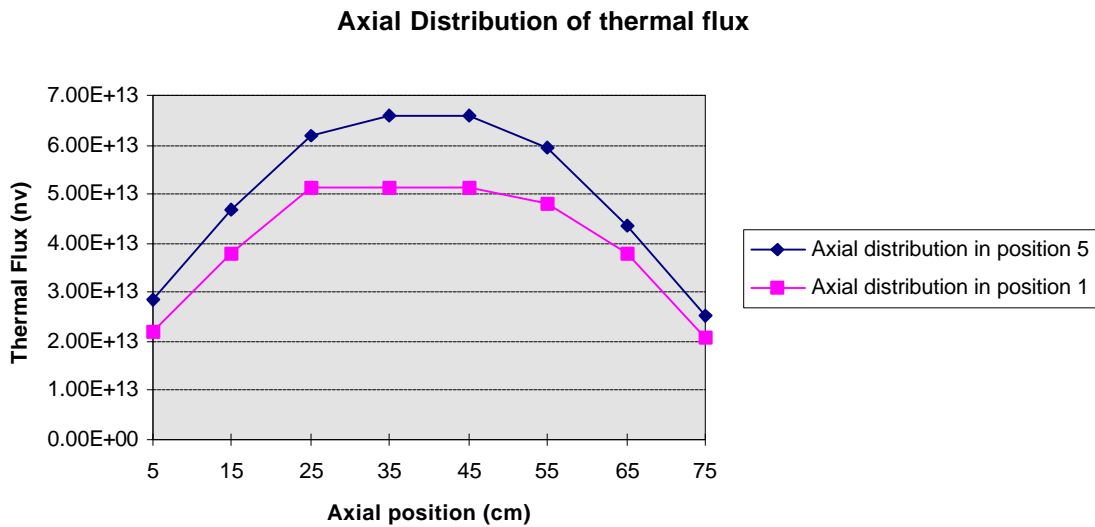


**Figure 5: Axial distribution of thermal flux in two detectors positions for the cobalt-box**

### Comparison Calculus-Experiment

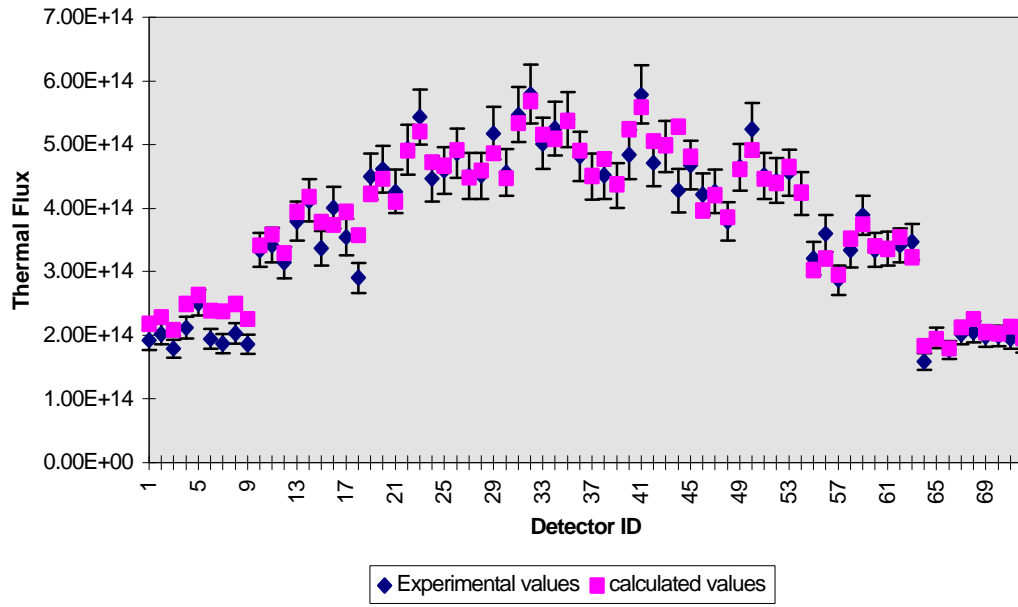


**Figure 6: Comparison between experimental and calculated data in the cobalt-box**

**Table 1.** Position of samples in Irradiation No. 1

<b>Irradiation No. 1</b>		Operation Time: 3Hs.		Date:8/Feb/98
Start Time: 12:37		CIC No. 1 = $1.0 \cdot 10^7$		
CR Position: 100 - 58.1 -100 - 0.0 - 100 - 0.0				
Plate Number	Fuel	Channel Number	Detector Number	Plate Position
2	A1	2	3-4-5-6	6-8-10-11
3	A1	10	8	8
4	A2	10	9-10-11	7-8
5	A3	10	12	8
6	A4	10	13	8
7	A5	10	14	8
8	C1	10	15-16-17	7-8-9
9	C1	2	18	8
10	C2	10	19	8
11	C3	10	20-21-22	7-8-9
12	C4	10	24-25-26-27-28	5-6-8-10-11
13	C5	10	30	8
14	E1	10	31	8
15	E2	10	32	8
16	E3	10	33-34-35	7-8-9
17	E4	10	36	8
18	E4	18	38-39-40-41-42	5-6-8-10-11
19	E5	10	44	8

**Table 2.** Position of samples in Irradiation No. 2

<b>Irradiation No. 2</b>		Operation Time: 3Hs.		Date:10/Feb/98
Start Time: 10:58		CIC No.1 = $1.1 \cdot 10^6$		
CR Position: 100 - 57.1 -100 - 0.0 - 100 - 0.0 <b>Under Cd</b>				
Plate Number	Fuel	Channel Number	Detector Number	Plate Position
3	E1	10	66	8
4	E4	18	70-71-72-74-75	5-6-8-10-11
5	C4	10	76	8 (MONITOR)
6	E2	10	67-68-69	7-9-13
9	A1	2	61	8
20	A4	10	62-63	7-9
21	C3	10	64-65	7-9

**Table 3.:** Position of samples in Irradiation No. 3

<b>Irradiation No. 3</b>		Operation Time: 1:13Hs.	Date:11/Feb/98	
Start Time: 12:10		CIC No.1 = $1.0 \cdot 10^6$		
CR Position: 100 - 57.5 -100 - 0.0 - 100 - 0.0				
Plate Number	Fuel	Channel Number	Detector Number	Plate Position
2	B1	10	45	8
7	B2	10	46	8
8	B3	10	47-48-49	7-8-9
10	B4	10	50	8
11	B5	2	52-53	8-11
12	D1	10	54	8
13	D2	10	55	8
14	D2	18	56	8
15	D4	10	57	8
16	D5	10	58	8
17	F1	10	59	8
18	F2	10	77-78-79-80-81-82	5-6-8-10-11
19	F3	10	84	8
5	C4	10	86	8(MONITOR)



**Table 4.** Thermal activities and calculated fluxes

Fuel Position <sup>(*)</sup>	A <sub>Bare</sub>	A <sub>Thermal</sub>	Calculated Fluxes	Fuel mass	A <sub>Thermal</sub> Normalised	Fluxes Normalised
A1-C2-6	2.66·10 <sup>7</sup>	9.57·10 <sup>6</sup>	6.40·10 <sup>13</sup>	405.75	1.51	1.83
A1-C2-8	3.47·10 <sup>7</sup>	1.25·10 <sup>7</sup>	8.00·10 <sup>13</sup>	405.75	1.97	2.29
A1-C2-10	3.81·10 <sup>7</sup>	1.37·10 <sup>7</sup>	8.00·10 <sup>13</sup>	405.75	2.16	2.29
A1-C2-11	3.29·10 <sup>7</sup>	1.18·10 <sup>7</sup>	6.60·10 <sup>13</sup>	405.75	1.87	1.89
A1-C10-8	4.80·10 <sup>7</sup>	1.19·10 <sup>7</sup>	7.40·10 <sup>13</sup>	405.75	1.87	2.12
A2-C10-7	8.37·10 <sup>7</sup>	2.84·10 <sup>7</sup>	1.38·10 <sup>14</sup>	209.24	2.31	2.04
A2-C10-8	7.09·10 <sup>7</sup>	2.40·10 <sup>7</sup>	1.30·10 <sup>14</sup>	209.24	1.95	1.92
A3-C10-8	7.11·10 <sup>7</sup>	2.41·10 <sup>7</sup>	1.33·10 <sup>14</sup>	209.24	1.96	1.97
A4-C10-8	4.75·10 <sup>7</sup>	1.61·10 <sup>7</sup>	1.01·10 <sup>14</sup>	209.24	1.31	1.49
A5-C10-8	2.65·10 <sup>7</sup>	6.57·10 <sup>6</sup>	4.70·10 <sup>13</sup>	405.75	1.04	1.35
B1-C10-8	6.39·10 <sup>7</sup>	2.17·10 <sup>7</sup>	1.18·10 <sup>14</sup>	209.24	1.76	1.74
B2-C10-8	7.27·10 <sup>7</sup>	2.46·10 <sup>7</sup>	1.58·10 <sup>14</sup>	209.24	2.00	2.33
B3-C10-7	1.02·10 <sup>8</sup>	4.47·10 <sup>7</sup>	1.99·10 <sup>14</sup>	146.3	2.54	2.06
B3-C10-8	9.00·10 <sup>7</sup>	3.96·10 <sup>7</sup>	1.90·10 <sup>14</sup>	146.3	2.25	1.96
B3-C10-9	8.87·10 <sup>7</sup>	3.90·10 <sup>7</sup>	1.68·10 <sup>14</sup>	146.3	2.22	1.74
B4-C10-8	6.76·10 <sup>7</sup>	2.97·10 <sup>7</sup>	1.47·10 <sup>14</sup>	146.3	1.69	1.52
B5-C2-8	2.81·10 <sup>7</sup>	9.53·10 <sup>6</sup>	5.60·10 <sup>13</sup>	209.24	0.77	0.83
B5-C2-11	2.94·10 <sup>7</sup>	9.96·10 <sup>6</sup>	4.40·10 <sup>13</sup>	209.24	0.81	0.65
C1-C10-7	7.51·10 <sup>7</sup>	2.55·10 <sup>7</sup>	1.11·10 <sup>14</sup>	209.24	2.07	1.64
C1-C10-8	6.81·10 <sup>7</sup>	2.31·10 <sup>7</sup>	1.10·10 <sup>14</sup>	209.24	1.88	1.63
C1-C10-9	5.42·10 <sup>7</sup>	1.84·10 <sup>7</sup>	1.15·10 <sup>14</sup>	209.24	1.50	1.70
C1-C2-8	5.55·10 <sup>7</sup>	1.86·10 <sup>7</sup>	1.21·10 <sup>14</sup>	209.24	1.51	1.79
C2-C10-8	9.80·10 <sup>7</sup>	4.31·10 <sup>7</sup>	1.83·10 <sup>14</sup>	146.3	2.45	1.89
C3-C10-7	1.09·10 <sup>8</sup>	5.39·10 <sup>7</sup>	3.10·10 <sup>14</sup>	146.3	3.06	3.20
C3-C10-8	9.85·10 <sup>7</sup>	4.50·10 <sup>7</sup>	2.21·10 <sup>14</sup>	146.3	2.56	2.28
C3-C10-9	1.00·10 <sup>8</sup>	4.42·10 <sup>7</sup>	2.04·10 <sup>14</sup>	146.3	2.51	2.11
C4-C10-5	4.52·10 <sup>7</sup>	1.99·10 <sup>7</sup>	9.90·10 <sup>13</sup>	146.3	1.13	1.02
C4-C10-6	6.96·10 <sup>7</sup>	3.06·10 <sup>7</sup>	1.54·10 <sup>14</sup>	146.3	1.74	1.59
C4-C10-8	7.64·10 <sup>7</sup>	3.36·10 <sup>7</sup>	1.80·10 <sup>14</sup>	146.3	1.91	1.86
C4-C10-10	7.25·10 <sup>7</sup>	3.19·10 <sup>7</sup>	1.77·10 <sup>14</sup>	146.3	1.81	1.83
C4-C10-11	5.53·10 <sup>7</sup>	2.43·10 <sup>7</sup>	1.41·10 <sup>14</sup>	146.3	1.38	1.46
C5-C10-8	4.46·10 <sup>7</sup>	1.51·10 <sup>7</sup>	1.05·10 <sup>14</sup>	209.24	1.23	1.55
D1-C10-8	6.64·10 <sup>7</sup>	2.25·10 <sup>7</sup>	1.15·10 <sup>14</sup>	209.24	1.83	1.70
D2-C10-8	9.91·10 <sup>7</sup>	4.36·10 <sup>7</sup>	2.03·10 <sup>14</sup>	146.3	2.48	2.10
D2-C18-8	1.06·10 <sup>8</sup>	5.24·10 <sup>7</sup>	3.02·10 <sup>14</sup>	146.3	2.98	3.12
D4-C10-8	8.13·10 <sup>7</sup>	3.58·10 <sup>7</sup>	1.95·10 <sup>14</sup>	146.3	2.03	2.01
D5-C10-8	4.45·10 <sup>7</sup>	1.64·10 <sup>7</sup>	1.07·10 <sup>14</sup>	209.24	1.33	1.58
E1-C10-8	6.80·10 <sup>7</sup>	1.68·10 <sup>7</sup>	9.70·10 <sup>13</sup>	405.75	2.65	2.78
E2-C10-8	9.58·10 <sup>7</sup>	3.25·10 <sup>7</sup>	1.77·10 <sup>14</sup>	209.24	2.64	2.62
E3-C10-7	1.18·10 <sup>8</sup>	5.19·10 <sup>7</sup>	3.00·10 <sup>14</sup>	146.3	2.95	3.10
E3-C10-8	1.01·10 <sup>8</sup>	4.45·10 <sup>7</sup>	2.23·10 <sup>14</sup>	146.3	2.53	2.30
E3-C10-9	1.00·10 <sup>8</sup>	4.40·10 <sup>7</sup>	1.89·10 <sup>14</sup>	146.3	2.50	1.95
E4-C10-8	5.98·10 <sup>7</sup>	2.03·10 <sup>7</sup>	1.38·10 <sup>14</sup>	209.24	1.65	2.04
E4-C18-5	2.19·10 <sup>7</sup>	6.34·10 <sup>6</sup>	4.20·10 <sup>13</sup>	209.24	0.52	0.62
E4-C18-6	3.52·10 <sup>7</sup>	1.02·10 <sup>7</sup>	6.30·10 <sup>13</sup>	209.24	0.83	0.93
E4-C18-8	4.56·10 <sup>7</sup>	1.32·10 <sup>7</sup>	7.30·10 <sup>13</sup>	209.24	1.07	1.08
E4-C18-10	4.51·10 <sup>7</sup>	1.30·10 <sup>7</sup>	7.10·10 <sup>13</sup>	209.24	1.06	1.05
E4-C18-11	3.86·10 <sup>7</sup>	1.11·10 <sup>7</sup>	5.70·10 <sup>13</sup>	209.24	0.91	0.84
E5-C10-8	4.02·10 <sup>7</sup>	1.31·10 <sup>7</sup>	8.20·10 <sup>13</sup>	209.24	1.07	1.21
F1-C10-8	5.80·10 <sup>7</sup>	1.43·10 <sup>7</sup>	9.10·10 <sup>13</sup>	405.75	2.26	2.61
F2-C10-8	7.63·10 <sup>7</sup>	1.89·10 <sup>7</sup>	1.14·10 <sup>14</sup>	405.75	2.98	3.27

Fuel Position <sup>(*)</sup>	A <sub>Bare</sub>	A <sub>Thermal</sub>	Calculated Fluxes	Fuel mass	A <sub>thermal</sub> Normalised	Fluxes Normalised
F3-C10-8	$7.84 \cdot 10^7$	$2.56 \cdot 10^7$	$1.54 \cdot 10^{14}$	209.24	2.08	2.28
F2-C10-10	$7.42 \cdot 10^7$	$1.83 \cdot 10^7$	$1.13 \cdot 10^{14}$	405.75	2.89	3.24

<sup>(\*)</sup> A1-C2-10 means fuel in A1 position, plate in Channel 2 and sample in position 10 in plate.

**Table 5:** Thermal Flux in each plane and in each measurement point

Plane A		
2.04E+13	2.30E+13	2.19E+13
2.21E+13	2.85E+13	2.41E+13
2.11E+13	2.31E+13	2.12E+13
<b>Control room</b>		

Plane B		
3.57E+13	3.88E+13	3.80E+13
3.83E+13	4.68E+13	4.31E+13
3.30E+13	4.03E+13	4.56E+13
<b>Control Room</b>		

Plane C		
4.84E+13	5.24E+13	5.11E+13
5.07E+13	6.18E+13	5.59E+13
5.12E+13	5.53E+13	5.21E+13
<b>Control Room</b>		

Plane D		
5.18E+13	5.89E+13	5.13E+13
5.70E+13	6.58E+13	6.21E+13
5.47E+13	6.12E+13	5.96E+13
<b>Control Room</b>		

Plane E		
4.95E+13	5.13E+13	5.12E+13
5.36E+13	6.57E+13	5.50E+13
5.32E+13	4.86E+13	5.65E+13
<b>Control Room</b>		

Plane F		
4.31E+13	4.84E+13	4.79E+13
5.13E+13	5.95E+13	5.28E+13
4.81E+13	5.17E+13	5.04E+13
<b>Control Room</b>		

Plane G		
3.26E+13	4.09E+13	3.64E+13
3.8E+13	4.41E+13	3.79E+13
3.94E+13	3.88E+13	3.82E+13
<b>Control Room</b>		

Plane H		
2.01E+13	2.22E+13	2.08E+13
2.24E+13	2.34E+13	2.3E+13
2.14E+13	1.99E+13	2.26E+13
<b>Control Room</b>		

**Table 6 :** Thermal flux at 2.5Mw for each sample in the cobalt-box

Sample and Position Identification	Thermal Flux (nv)	error	Sample and Position Identification	Thermal Flux (nv)	Error
a1	2.19E+13	1.9E+12	e1	5.12E+13	4.0E+12
a2	2.30E+13	2.0E+12	e2	5.13E+13	4.1E+12
a3	2.04E+13	1.8E+12	e3	4.95E+13	3.9E+12
a4	2.41E+13	2.1E+12	e4	5.50E+13	4.3E+12
a5	2.85E+13	2.5E+12	e5	6.57E+13	5.2E+12
a6	2.21E+13	1.9E+12	e6	5.36E+13	4.2E+12
a7	2.12E+13	1.9E+12	e7	5.65E+13	4.5E+12
a8	2.31E+13	2.0E+12	e8	4.86E+13	3.8E+12
a9	2.11E+13	1.9E+12	e9	5.32E+13	4.2E+12
b1	3.80E+13	3.0E+12	f1	4.79E+13	3.8E+12
b2	3.88E+13	3.1E+12	f2	4.84E+13	3.8E+12
b3	3.57E+13	2.8E+12	f3	4.31E+13	3.4E+12
b4	4.31E+13	3.4E+12	f4	5.28E+13	4.2E+12
b5	4.68E+13	3.7E+12	f5	5.95E+13	4.7E+12
b6	3.83E+13	3.0E+12	f6	5.13E+13	4.1E+12
b7	4.56E+13	3.6E+12	f7	5.04E+13	4.0E+12
b8	4.03E+13	3.2E+12	f8	5.17E+13	4.1E+12
b9	3.30E+13	2.6E+12	f9	4.81E+13	3.8E+12
c1	5.11E+13	4.0E+12	g1	3.64E+13	2.9E+12
c2	5.24E+13	4.1E+12	g2	4.09E+13	3.2E+12
c3	4.84E+13	3.8E+12	g3	3.26E+13	2.6E+12
c4	5.59E+13	4.4E+12	g4	3.79E+13	3.0E+12
c5	6.18E+13	4.9E+12	g5	4.41E+13	3.5E+12
c6	5.07E+13	4.0E+12	g6	3.80E+13	3.0E+12
c7	5.21E+13	4.1E+12	g7	3.82E+13	3.0E+12
c8	5.53E+13	4.4E+12	g8	3.88E+13	3.1E+12
c9	5.12E+13	4.1E+12	g9	3.94E+13	3.1E+12
d1	5.13E+13	4.1E+12	h1	1.81E+13	1.6E+12
d2	5.89E+13	4.7E+12	h2	2.22E+13	2.0E+12
d3	5.18E+13	4.1E+12	h3	2.01E+13	1.8E+12
d4	6.21E+13	4.9E+12	h4	2.30E+13	2.0E+12
d5	6.58E+13	5.2E+12	h5	2.34E+13	2.1E+12
d6	5.70E+13	4.5E+12	h6	2.24E+13	2.0E+12
d7	5.96E+13	4.7E+12	h7	2.26E+13	2.0E+12
d8	6.12E+13	4.9E+12	h8	2.21E+13	1.9E+12
d9	5.47E+13	4.3E+12	h9	2.14E+13	1.9E+12

<b>Id. Position</b>	<b>Thermal Flux Experimental</b>	<b>Thermal Flux Calculation</b>	<b>Calc./exp</b>	<b>Id. Position</b>	<b>Thermal Flux Experimental</b>	<b>Thermal Flux Calculation</b>	<b>Calc./exp</b>
<b>a1</b>	1.93E+14	2.18E+14	0.88	<b>e1</b>	4.50E+14	4.50E+14	1.00
<b>a2</b>	2.02E+14	2.29E+14	0.88	<b>e2</b>	4.51E+14	4.77E+14	0.95
<b>a3</b>	1.79E+14	2.09E+14	0.86	<b>e3</b>	4.36E+14	4.38E+14	1.00
<b>a4</b>	2.12E+14	2.50E+14	0.85	<b>e4</b>	4.84E+14	5.24E+14	0.92
<b>a5</b>	2.51E+14	2.64E+14	0.95	<b>e5</b>	5.78E+14	5.58E+14	1.04
<b>a6</b>	1.95E+14	2.39E+14	0.82	<b>e6</b>	4.72E+14	5.06E+14	0.93
<b>a7</b>	1.87E+14	2.38E+14	0.78	<b>e7</b>	4.97E+14	4.99E+14	1.00
<b>a8</b>	2.03E+14	2.49E+14	0.82	<b>e8</b>	4.27E+14	5.28E+14	0.81
<b>a9</b>	1.86E+14	2.26E+14	0.82	<b>e9</b>	4.68E+14	4.81E+14	0.97
<b>b1</b>	3.34E+14	3.41E+14	0.98	<b>f1</b>	4.21E+14	3.96E+14	1.06
<b>b2</b>	3.42E+14	3.59E+14	0.95	<b>f2</b>	4.26E+14	4.20E+14	1.01
<b>b3</b>	3.14E+14	3.29E+14	0.96	<b>f3</b>	3.79E+14	3.86E+14	0.98
<b>b4</b>	3.80E+14	3.94E+14	0.96	<b>f4</b>	4.65E+14	4.61E+14	1.01
<b>b5</b>	4.12E+14	4.18E+14	0.99	<b>f5</b>	5.24E+14	4.91E+14	1.07
<b>b6</b>	3.37E+14	3.78E+14	0.89	<b>f6</b>	4.51E+14	4.46E+14	1.01
<b>b7</b>	4.01E+14	3.74E+14	1.07	<b>f7</b>	4.43E+14	4.40E+14	1.01
<b>b8</b>	3.55E+14	3.94E+14	0.90	<b>f8</b>	4.55E+14	4.65E+14	0.98
<b>b9</b>	2.91E+14	3.58E+14	0.81	<b>f9</b>	4.23E+14	4.24E+14	1.00
<b>c1</b>	4.50E+14	4.22E+14	1.07	<b>g1</b>	3.21E+14	3.03E+14	1.06
<b>c2</b>	4.61E+14	4.46E+14	1.03	<b>g2</b>	3.60E+14	3.21E+14	1.12
<b>c3</b>	4.26E+14	4.10E+14	1.04	<b>g3</b>	2.87E+14	2.95E+14	0.97
<b>c4</b>	4.92E+14	4.90E+14	1.00	<b>g4</b>	3.34E+14	3.52E+14	0.95
<b>c5</b>	5.43E+14	5.21E+14	1.04	<b>g5</b>	3.88E+14	3.75E+14	1.04
<b>c6</b>	4.46E+14	4.72E+14	0.95	<b>g6</b>	3.34E+14	3.40E+14	0.98
<b>c7</b>	4.59E+14	4.67E+14	0.98	<b>g7</b>	3.36E+14	3.36E+14	1.00
<b>c8</b>	4.87E+14	4.92E+14	0.99	<b>g8</b>	3.42E+14	3.54E+14	0.96
<b>c9</b>	4.51E+14	4.48E+14	1.01	<b>g9</b>	3.47E+14	3.23E+14	1.07
<b>d1</b>	4.51E+14	4.59E+14	0.98	<b>h1</b>	1.59E+14	1.84E+14	0.86
<b>d2</b>	5.18E+14	4.86E+14	1.07	<b>h2</b>	1.96E+14	1.94E+14	1.01
<b>d3</b>	4.56E+14	4.47E+14	1.02	<b>h3</b>	1.77E+14	1.79E+14	0.99
<b>d4</b>	5.47E+14	5.34E+14	1.02	<b>h4</b>	2.02E+14	2.13E+14	0.95
<b>d5</b>	5.79E+14	5.68E+14	1.02	<b>h5</b>	2.06E+14	2.26E+14	0.91
<b>d6</b>	5.02E+14	5.15E+14	0.97	<b>h6</b>	1.97E+14	2.05E+14	0.96
<b>d7</b>	5.25E+14	5.09E+14	1.03	<b>h7</b>	1.99E+14	2.03E+14	0.98
<b>d8</b>	5.39E+14	5.37E+14	1.00	<b>h8</b>	1.95E+14	2.14E+14	0.91
<b>d9</b>	4.82E+14	4.9E+14	0.98	<b>h9</b>	1.88E+14	1.95E+14	0.97

- /1/ Beckurtz and Wirtz, Neutron Physics
- /2/ Effective Cadmium Cutoff Energies, R. Stoughton, J. Halperin, M. Lietzke, Nuclear Science Engineering, 6, 441-447
- /3/ Flux Perturbation by Detectors Foils, Alain Sola, Nucleonics, 1960.
- /4/ INVAP Commissioning Procedure 0767-542-3PPGC-009-10
- /5/ G. Gennuso Internal Report
- /6/ IAEA, Tecdoc 107, Neutron Fluence Measurement
- /7/ Nuclear Data Guide for Reactor Neutron Metrology, J. H. Beard, W. L. Zijp, and H. J. Nolthenius, Kluwer Academic Publisher
- /8/ DIN/GN/001-96 New isotopes in the WIMS library.
- /9/ A general description of the lattice code WIMS, Askew, Fayers & Kemshell, UKAEA, 1967.
- /10/ POS\_WIMS. MTR\_PC User manual. Julio 1993.
- /11/ CITVAP 3.1. MTR\_PC 2.6 User Manual. Julio 1995.
- /12/ HXS 4.0 MTR\_PC 2.6 User manual. Julio 1995.